Supporting Information

Nanosized Metal-Organic Framework Confined inside Functionalized Mesoporous Polymer: An Efficient CO_2 Adsorbent with Metal Defects

Chengli Jiao,[ab] *Zeeshan Majeed,*[a] *Guang-Hui Wang,*[a] *and Heqing Jiang**[ab]

[a]Qingdao Key Laboratory of Functional Membrane Material and Membrane Technology, Qingdao Institute of Bioenergy and Bioprocess Technology, Chinese Academy of Sciences, No.189 Songling Road, 266101 Qingdao (China)

[b]Dalian National Laboratory for Clean Energy, Dalian Institute of Chemical Physics, Chinese Academy of Sciences , 457 Zhongshan Road, 116023 Dalian (China)

Corresponding Author* Email: jianghq@qibebt.ac.cn

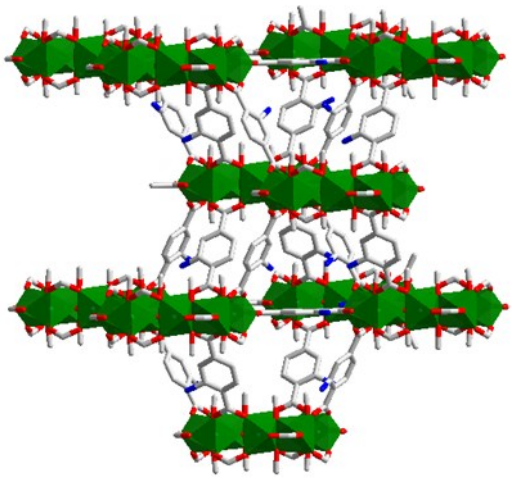

Fig. S1 Crystal structure of CAU-1. Hydrogen are omitted for clarity. C, gray; O, red; N, blue; {AlO_6} octahedra, green.

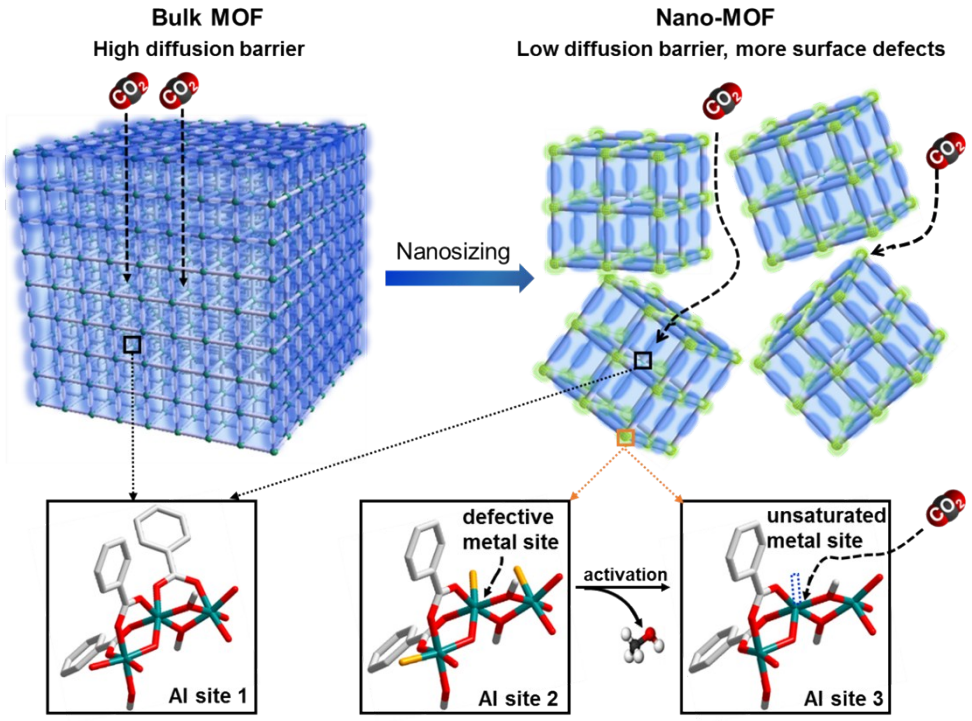

Fig. S2 Differences between bulk MOF and nano-MOF. For clarity, hydrogen and nitrogen in CAU-1 are omitted. Al, green; C, gray; O of ligands the same as bulk MOF, red; and O of terminated ligands, orange for CAU-1.

Bulk MOF has a high diffusion barrier resulted from the possible pore blockage through the long diffusion paths of guest molecule. When MOF crystal is scaled down to nanoscale range, the diffusion paths are dramatically shortened, which results in a low diffusion barrier and a fast mass transfer. Additionally, for bulk CAU-1 even after activation, saturated Al metal center is in an octahedral coordination geometry, and six-coordinated by three carboxylate oxygen atoms from ligands, two bridging methoxide ions and one bridging hydroxide (Al site 1). The relative number of surface Al site will drastically increase when CAU-1 crystals are scaled down to the nanoscale range. Different to the Al center (Al site 1) in the bulk part, Al center on the surface (Al site 2) will be terminated by partially coordinated ligands, methanol, hydroxide or carbonyl oxygen atoms from FMP. The terminated reagents (such as methanol) of Al site 2 can be removed via thermal activation, leading to the formation of coordinatively unsaturated metal site (Al site 3).

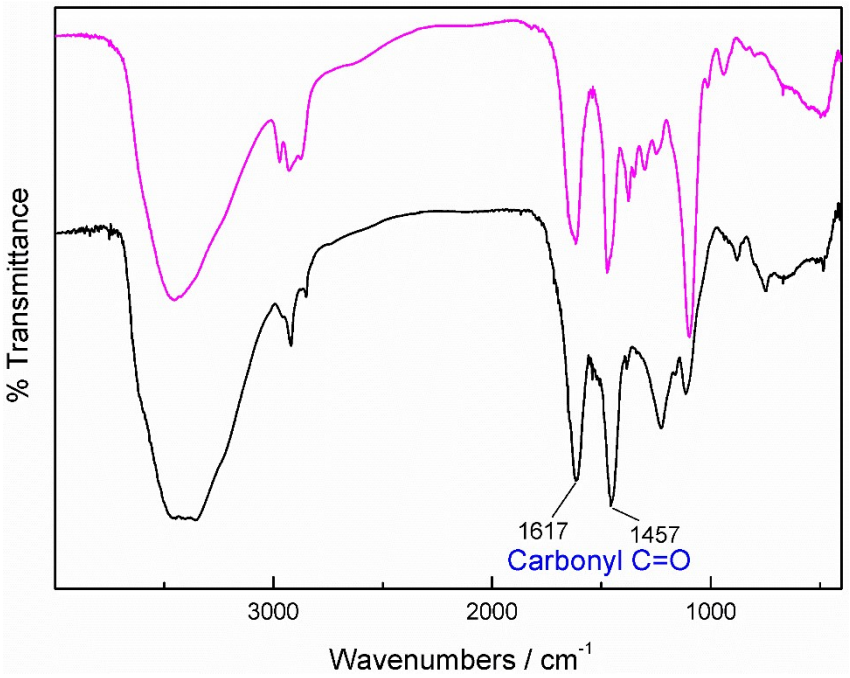

Fig. S3 FT-IR spectra of FMP (black) and FMP precursor before activation at 350 °C (pink).

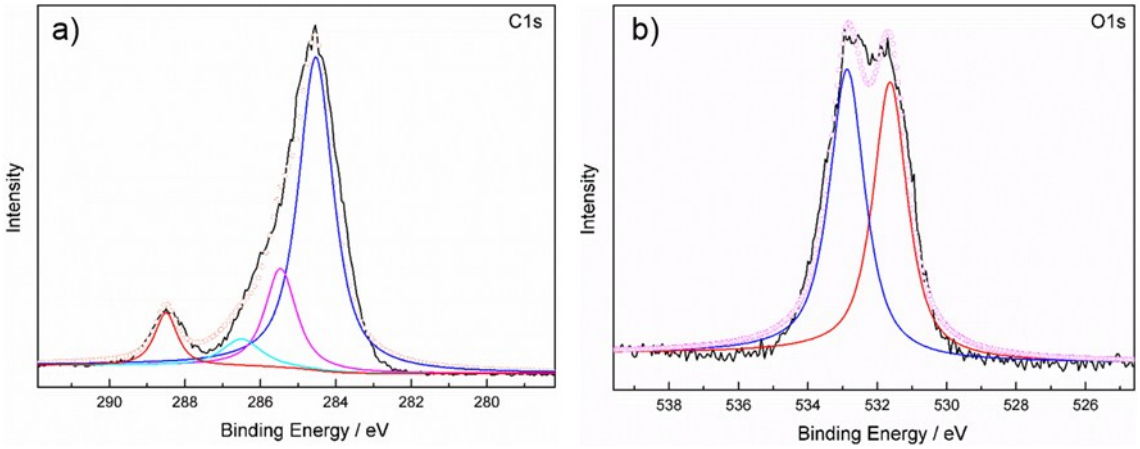

Fig. S4 a) C1s and b) O1s XPS spectra of FMP.

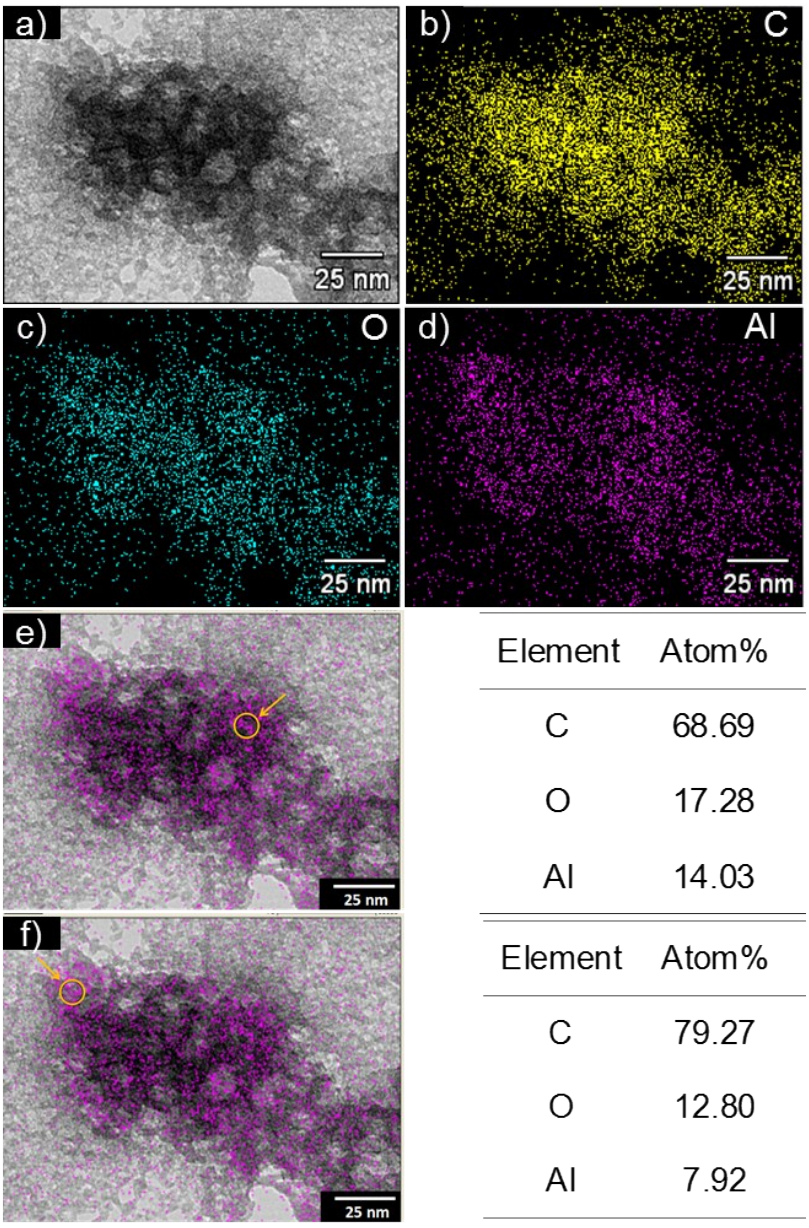

Element	Atom%
C	68.69
O	17.28
Al	14.03

Element	Atom%
C	79.27
O	12.80
Al	7.92

Fig. S5 a) STEM image, b-d) corresponding elemental mapping, (e and f) EDX analysis of CAU-1@FMP.

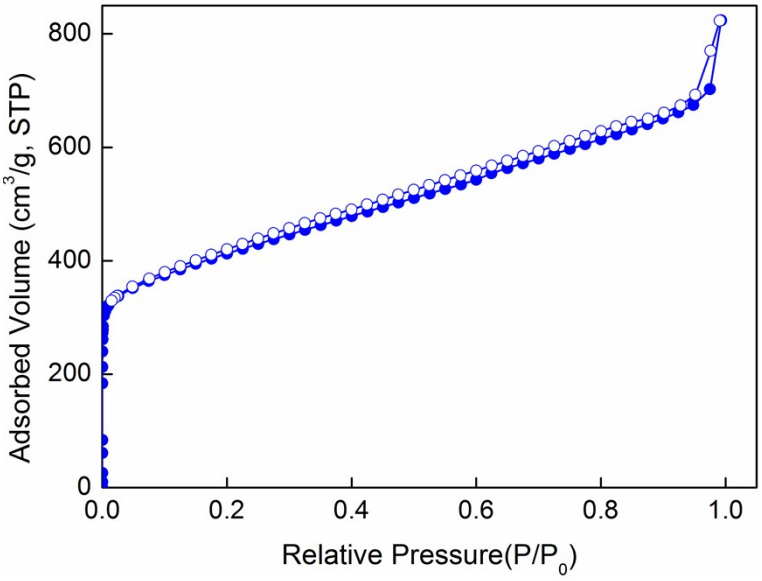

Fig. S6 Nitrogen adsorption-desorption isotherms at 77 K of CAU-1.

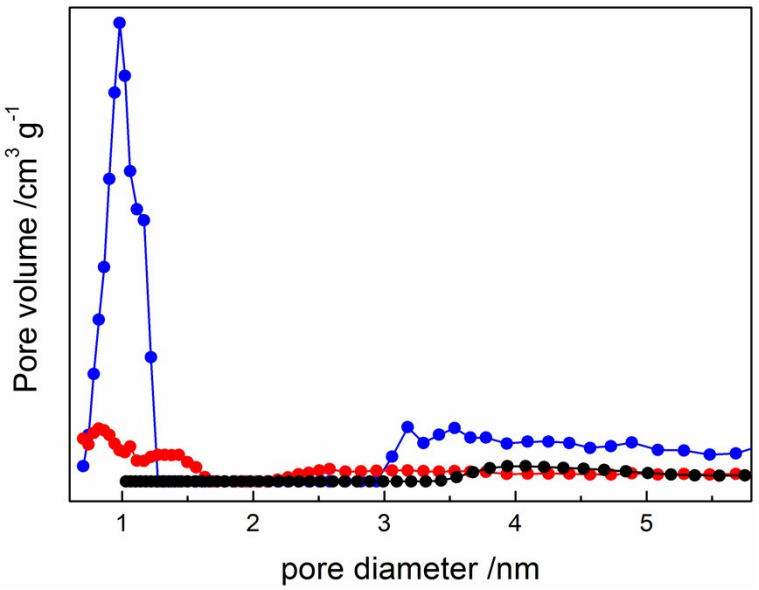

Fig. S7 Pore size distribution of FMP (black), CAU-1@FMP (red) and CAU-1 (blue), calculated using density functional theory (DFT) analysis.

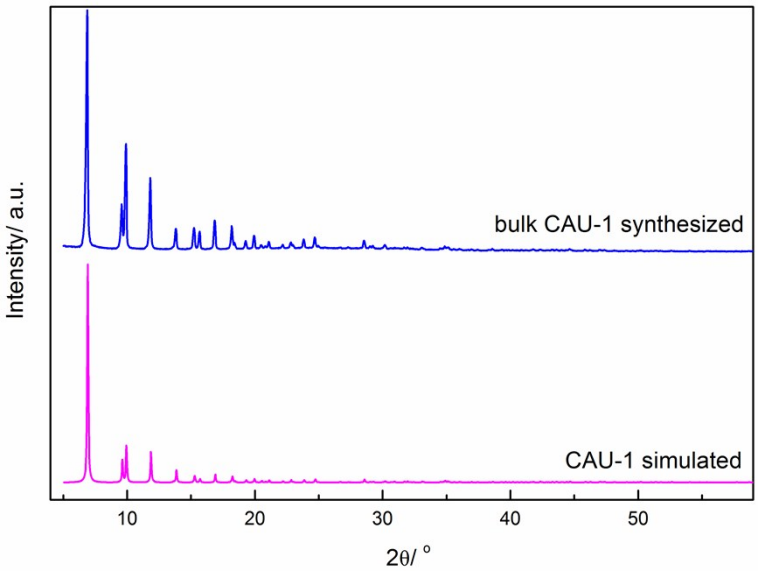

Fig. S8 Simulated XRD pattern for CAU-1 and measured PXRD patterns for bulk CAU-1 synthesized.

Table S1 Parameters of the porous structures of FMP, CAU-1 and CAU-1@FMP.

Sample	BET surface area (m^2 g^{-1})	Micropore volume (cm^3 g^{-1})	Total pore volume (cm^3 g^{-1})
FMP	195	0.01	0.40
CAU-1	1477	0.42	1.27
CAU-1@FMP	489	0.13	0.76

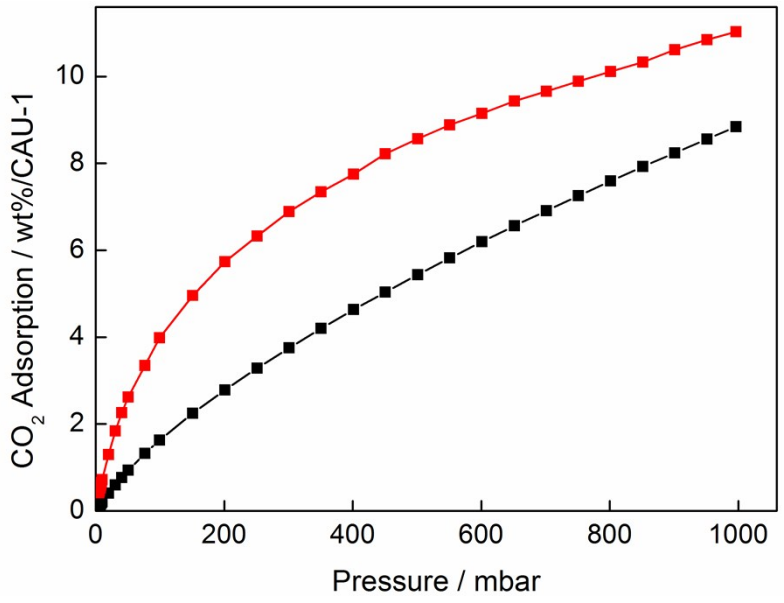

Fig. S9 CO_2 adsorption capacities (wt% CO_2/ CAU-1) of CAU-1 (black), CAU-1@FMP (red) at 298 K. The adsorption capacity of CAU-1@FMP was calculated by subtracting the uptake of FMP substrate from the measured uptake.

Table S2 CO_2 adsorption capacities in metal organic frameworks. The highest and the second highest values at 273 K were highlighted in blue and green, respectively. The highest and the second highest values at 298 K were highlighted in red and pink, respectively.

MOF		CO_2 adsorption capacity (wt% / MOF)			Reference
Chemical formula	Common	150 mbar	1000 mbar	Temperature (K)	
Confined CAU-1 in FMP		16.0	27.5	273	This work
		5.0	11.0	298	
Bulk CAU-1		4.0	16.2	273	This work
		2.2	8.8	298	
Confined MOP-SO_3H in SBA-16 (MOP content ~6.4 wt%)		8.0	28.9	273	S1
Confined MOP-SO_3H in SBA-16 (MOP content ~12.02 wt%)		4.2	12.8	273	S1
HKUST-1 in SBA-15 (HKUST-1 content~97.19 wt%)		4.6	17.9	298	S2
Ni_2(dobdc)	Ni-MOF-74	14.1	20.5	273	S3
		10.6	17.4	298	S3
$[Cu_2(BDPT^{4-})]_n$	HNUST-5	4.9	15.8	273	S4
Zn_2(dobdc)	Zn-MOF-74	10.4	21.4	273	S3
Cu_2(EBTC)		8.1	25.9	273	S5
		4.46	14.1	298	S5
$Cu_3(BTC)_2$	HKUST-1	7.9	31.7	273	S6
		2.0	18.4	298	S7
$Cu_2(abtc)_3$	SNU-5	6.9	38.5	273	S8
$Cu_2(C_{22}H_{10}O_8)(H_2O)_2$	NOTT-101	5.7	23.8	273	S9
Cu-TTTT	HNUST-1	10.6	23.5	273	S10
		4.3	12.6	298	S10
$Zn(Pur)_2$	ZIF-20	4.7	12.4	273	S11
[Cu(bpy)$_2$(EDS)]n	TMOF-1	4.3	8.4	273	S12
$Cu_2(BPnDC)_2(bpy)$	SNU-6	3.8	9.9	273	S13
$[(CH_3)_2NH_2]_2[Zn_3(TADIPA)_2(DMF)_2]$	JLU-Liu40	3.6	20.7	273	S14
Zn(nIM)(5cbIM)	ZIF-69	3.3	11.8	273	S15
$Cu_2(CNBPDC)_2\cdot(DMF)_2$	MOF-601	3.2	7.4	273	S16
$\{[Cu(azbpy)(2ntp)]\cdot H_2O\}n$		2.4	7.9	273	S17
$Zn_4O(BDC)_3$	MOF-5, IRMOF-1	1.8	6.2	273	S18
		1.1	3.5	298	S19
$Cu_2(IBPDC)_2\cdot(Py)_{1.67}(H_2O)_{0.33}$	MOF-603	1.4	4.9	273	S20
$Zn(mIM)_2$	ZIF-8	1.1	6.8	273	S21
		0.6	3.8	298	S21

References

S1. Y.-H. Kang, X.-D. Liu, N. Yan, Y. Jiang, X.-Q. Liu, L.-B. Sun and J.-R. Li, *J. Am. Chem. Soc.*, 2016, **138**, 6099-6102.

S2. C. Chen, B. Li, L. Zhou, Z. Xia, N. Feng, J. Ding, L. Wang, H. Wan and G. Guan, *ACS Appl. Mater. Inter.*, 2017, **9**, 23060-23071.

S3. G. Y. Yoo, W. R. Lee, H. Jo, J. Park, J. H. Song, K. S. Lim, D. Moon, H. Jung, J. Lim, S. S. Han, Y. Jung and C. S. Hong, *Chem. Eur. J.*, 2016, **22**, 7444-7451.

S4. B. Zheng, H. Liu, Z. Wang, X. Yu, P. Yi and J. Bai, *Crystengcomm*, 2013, **15**, 3517-3520.

S5. Y. Hu, S. Xiang, W. Zhang, Z. Zhang, L. Wang, J. Bai and B. Chen, *Chem. Commun.*, 2009, 7551-7553.

S6. X. Yan, S. Komarneni, Z. Zhang and Z. Yan, *Microporous Mesoporous Mater.*, 2014, **183**, 69-73.

S7. A. O. Yazaydin, A. I. Benin, S. A. Faheem, P. Jakubczak, J. J. Low, R. R. Willis and R. Q. Snurr, *Chem. Mater.*, 2009, **21**, 1425-1430.

S8. Y.-G. Lee, H. R. Moon, Y. E. Cheon and M. P. Suh, *Angew. Chem. Int. Ed.*, 2008, **47**, 7741-7745.

S9. H.-M. Wen, H. Wang, B. Li, Y. Cui, H. Wang, G. Qian and B. Chen, *Inorg. Chem.*, 2016, **55**, 7214-7218.

S10. B. Zheng, H. Wang, Z. Wang, N. Ozaki, C. Hang, X. Luo, L. Huang, W. Zeng, M. Yang and J. Duan, *Chem. Commun.*, 2016, **52**, 12988-12991.

S11. H. Hayashi, A. P. Cote, H. Furukawa, M. O'Keeffe and O. M. Yaghi, *Nat. Mater.*, 2007, **6**, 501-506.

S12. G. Zhang, G. Wei, Z. Liu, S. R. J. Oliver and H. Fei, *Chem. Mater.*, 2016, **28**, 6276-6281.

S13. H. J. Park and M. P. Suh, *Chem. Eur. J.*, 2008, **14**, 8812-8821.

S14. Q. Sun, S. Yao, B. Liu, X. Liu, G. Li, X. Liu and Y. Liu, *Dalton Trans.*, 2018, **47**, 5005-5010.

S15. R. Banerjee, A. Phan, B. Wang, C. Knobler, H. Furukawa, M. O'Keeffe and O. M. Yaghi, *Science*, 2008, **319**, 939-943.

S16. H. Furukawa, J. Kim, N. W. Ockwig, M. O'Keeffe and O. M. Yaghi, *J. Am. Chem. Soc.*, 2008, **130**, 11650-11661.

S17. D. K. Maity, A. Halder, B. Bhattacharya, A. Das and D. Ghoshal, *Cryst. Growth Des.*, 2016, **16**, 1162-1167.

S18. K. S. Walton, A. R. Millward, D. Dubbeldam, H. Frost, J. J. Low, O. M. Yaghi and R. Q. Snurr, *J. Am. Chem. Soc.*, 2008, **130**, 406-407.

S19. D. Saha, Z. Bao, F. Jia and S. Deng, *Environ. Sci. Technol.*, 2010, **44**, 1820-1826.

S20. L. Pan, K. M. Adams, H. E. Hernandez, X. T. Wang, C. Zheng, Y. Hattori and K. Kaneko, *J. Am. Chem. Soc.*, 2003, **125**, 3062-3067.

S21. Y. Yang, L. Ge, V. Rudolph and Z. Zhu, *Dalton Trans.*, 2014, **43**, 7028-7036.